PTEP

Prog. Theor. Exp. Phys. **2012**, 04D003 (12 pages)
DOI: 10.1093/ptep/pts062

Precise measurement of positronium

Toshio Namba*

International Center for Elementary Particle Physics, University of Tokyo, 7-3-1 Hongo, Bunkyo, Tokyo 113-0033, Japan
*E-mail: naniwa@icepp.s.u-tokyo.ac.jp

Received October 11, 2012; Accepted November 5, 2012; Published December 17, 2012

Positronium is an ideal system for research into bound-state quantum electrodynamics. In this paper, many properties of positronium are precisely measured and compared with theory. Two properties, the lifetime of ortho-positronium and ground-state hyperfine splitting, are discussed.

1. Introduction

Positronium (Ps), the bound state of an electron and a positron, is a purely leptonic system and is a very light two-body atom similar to hydrogen. The properties of Ps are described by bound-state quantum electrodynamics (QED). The calculation of bound-state QED is not as easy as that of QED for free particles, because it describes a 'bound' system in which Coulomb exchange is not a small effect. To calculate this, a special treatment like a non-relativistic quantum electrodynamics (NRQED) approach is required; recently, many studies of Ps have contributed to the development of bound-state QED [1,2].

There are two important merits of using the Ps atom to study bound-state QED. One is that Ps is free from hadronic effects. Since Ps consists of two leptons, no uncertainty like the proton charge radius exists. Because of its lightness, hadronic momentum transfer, which can be seen in the muonium calculation, can also be ignored. Another merit of Ps measurement is that Ps is a pair consisting of a particle and its antiparticle. Their masses and magnetic moments are exactly the same, and there is no uncertainty about their ratio.

From the experimental point of view, the convenience of Ps creation is a great advantage. Only radioisotopes like ^{22}Na or ^{68}Ge–Ga are needed to create this simple matter–antimatter system, and no accelerators or reactors are required. Our group has studied Ps for more than 20 years as a probe to search for new physics beyond the standard model and to study bound-state QED precisely. Our studies are divided into two categories: one is the search for rare decay modes of Ps, to search for new physics beyond the standard model. Since Ps is at the low-energy limit of e^+ e^- colliders, its rare decay search is sensitive to a new light particle with very weak couplings. Various searches have been done by many groups [3–17]. The other category is the precision measurement of Ps properties to study bound-state QED. In this paper, we focus on the precision measurements of Ps, and show our two experiments, the measurement of the lifetime of ortho-positronium (o-Ps) and the measurement of the hyperfine splitting of ground-state Ps.

2. Lifetime measurement of ortho-positronium

Two ground states of Ps, the triplet 1^3S_1 state (o-Ps) and the singlet 1^1S_0 state (para-positronium, p-Ps) give a clear demonstration of the C-parity conservation law. p-Ps has an 'even' eigenstate under

C conjugation; it decays to even γ rays, mainly to two 511 keV back-to-back monochromatic γ rays. o-Ps has an 'odd' eigenstate, and it decays to odd γ rays, mainly to three continuous-energy γ rays.

The lifetime of p-Ps was precisely measured in 1994 by using a magnetic mixing method [18]. The experimental value is

$$\tau_{\text{p-Ps}} = 1/\Gamma_{\text{p-Ps}} = 1/(7990.9 \pm 1.7\,\mu\text{s}^{-1}) \simeq 125.1\,\text{ps}, \tag{1}$$

which is in good agreement with the theoretical calculation [19,20], $\Gamma_{\text{p-Ps}} = 7989.62(4)\,\mu\text{s}^{-1}$, within an experimental error of 200 ppm.

On the other hand, the lifetime of o-Ps ($\tau_{\text{o-Ps}} \simeq 142\,\text{ns}$) is larger than that of p-Ps by about three orders of magnitude, because of three-body decay. In the first half of the 1990s, there was a long-standing problem, called the 'o-Ps lifetime puzzle'. Three precise measurements [22–24] of the o-Ps decay rate were performed by the Michigan group, and all reported a much larger decay rate—by around 1000 ppm—than the QED prediction. In an effort to clarify the discrepancy, various exotic decay modes have been searched for, without any evidence [7–17].

This 'o-Ps lifetime puzzle' was solved in 1995 by our group [21]. The key to solving it was the 'pickoff' annihilation during the thermalization process of Ps. Since the binding energy of Ps is 6.8 eV, Ps has a kinetic energy of about 1 eV just after formation. The formed Ps slows and is cooled down toward a thermal energy of about 0.03 eV ('thermalization') by colliding with surrounding atoms. In this process, some portion of the Ps inevitably causes pickoff annihilation with the atomic electrons. The observed o-Ps decay rate λ_{obs} is a sum of the intrinsic o-Ps decay rate $\lambda_{3\gamma}$ and the pickoff annihilation rate λ_{pick}, i.e.

$$\lambda_{\text{obs}}(t) = \lambda_{3\gamma} + \lambda_{\text{pick}}(t). \tag{2}$$

In all previous experiments, λ_{pick} was assumed to be constant; this assumption was wrong because the collision rate depends on the velocity of Ps, which slows down during the thermalization process.

Our group directly measured the pickoff rate with high energy-resolution germanium detectors and corrected its effect on the o-Ps lifetime. The experimental setup is shown in Fig. 1. A ^{68}Ge–Ga positron source with a strength of 11 kBq, being sandwiched between two sheets of plastic scintillators (trigger scintillators, NE102 thickness = 0.2 mm) and held by a cone made of aluminized mylar, is placed at the center of a glass beaker. The beaker is filled with SiO_2 aerogel or powder whose density is 0.03 g/cm^3, and evacuated down to 1×10^{-2} Torr. The surfaces of the SiO_2 grain are replaced with hydrophobic ones in order to remove the electric dipole of the OH-. The inner surface of the beaker is surrounded by 1 mm-thick plastic scintillators to veto the positron passing thorough the silica. Three high-purity coaxial germanium detectors (Ortec GEM38195) and four $50 \times 50 \times 33$ mm YAP ($YAlO_3$:Ce doped) scintillators are placed around the beaker.

The o-Ps lifetime spectrum is observed as the time difference between the signal from the trigger scintillators and that from the YAP scintillators (Fig. 2 (left)). In this spectrum, three components, the prompt peak at the timing origin in which the positron annihilations and p-Ps decays are contained, the accidental flat distribution, and the o-Ps decay curve including the pickoff events, are clearly seen. To estimate the pickoff effect, the energy spectrum obtained by the germanium detectors is used. Due to their high energy resolution, the 3γ spectrum emitted from o-Ps decay can be separated from the 2γ spectrum from the pickoff process with the germanium detectors. Our group carefully estimated the pickoff rate against the 3γ decay rate ($\lambda_{\text{pick}}/\lambda_{3\gamma}$) as a function of time, as shown in Fig. 2 (right). As shown, it takes a long time for the produced Ps to be well thermalized, and the

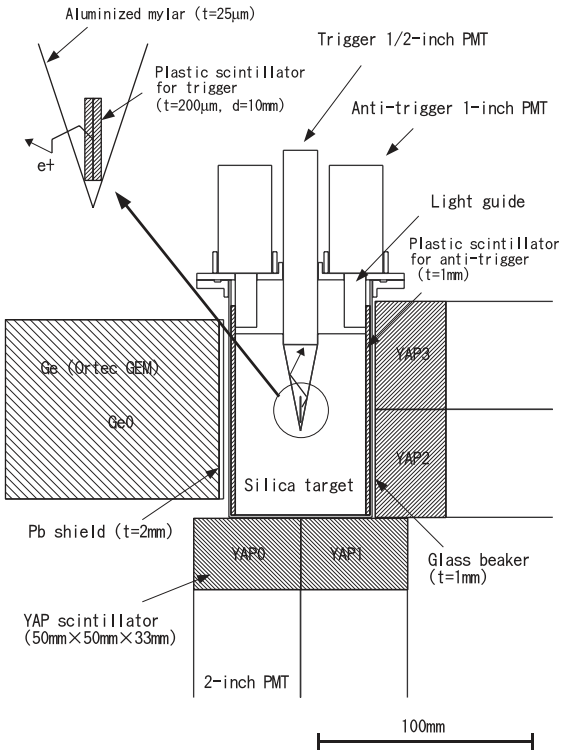

Fig. 1. The experimental setup for the lifetime measurement. Republished with permission from [28].

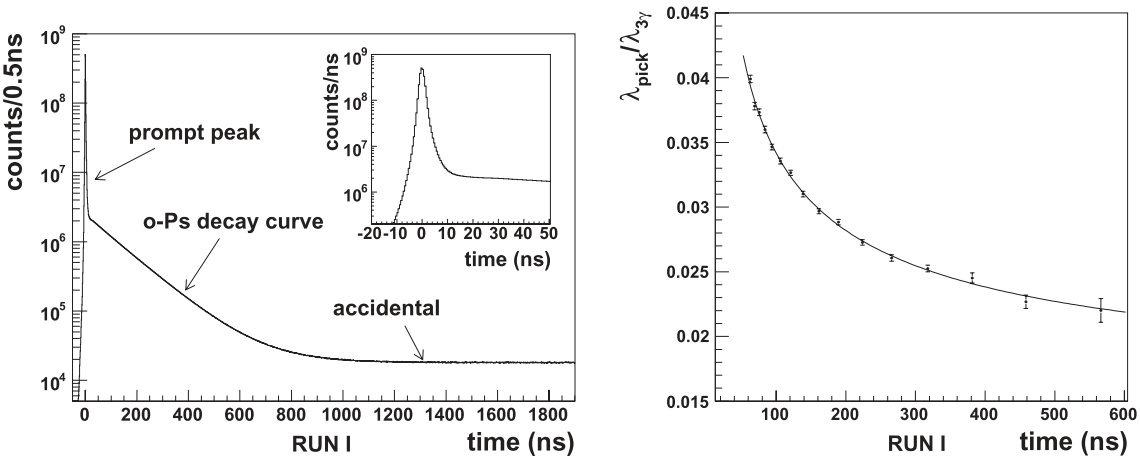

Fig. 2. (Left) Measured o-Ps timing spectrum with the YAP scintillators. (Right) Timing dependence of the pickoff rate. λ_{pick} changes slowly due to the slow thermalization process. Republished with permission from [28].

population of o-Ps at time t ($N(t)$) should be expressed as

$$N(t) = N_0 \exp\left\{-\lambda_{3\gamma}\int_0^t \left(1 + \frac{\lambda_{pick}(t')}{\lambda_{3\gamma}}\right) dt'\right\}. \tag{3}$$

Considering the detection efficiency and the random stopping rate correction, we fitted the o-Ps decay curve with Eq. (3). As a result, we solved the o-Ps lifetime puzzle, and we pinned down the decay width of o-Ps to 150 ppm accuracy, $\Gamma_{o\text{-}Ps} = 7.0401 \pm 0.0006(\text{stat.})^{+0.0007}_{-0.0009}(\text{sys.})\,\mu s^{-1}$ [27]. After the first measurement [21] of our group, the Michigan group performed another measurement [25]. They used a porous silica film optimized for the full thermalization of Ps as the Ps formation region,

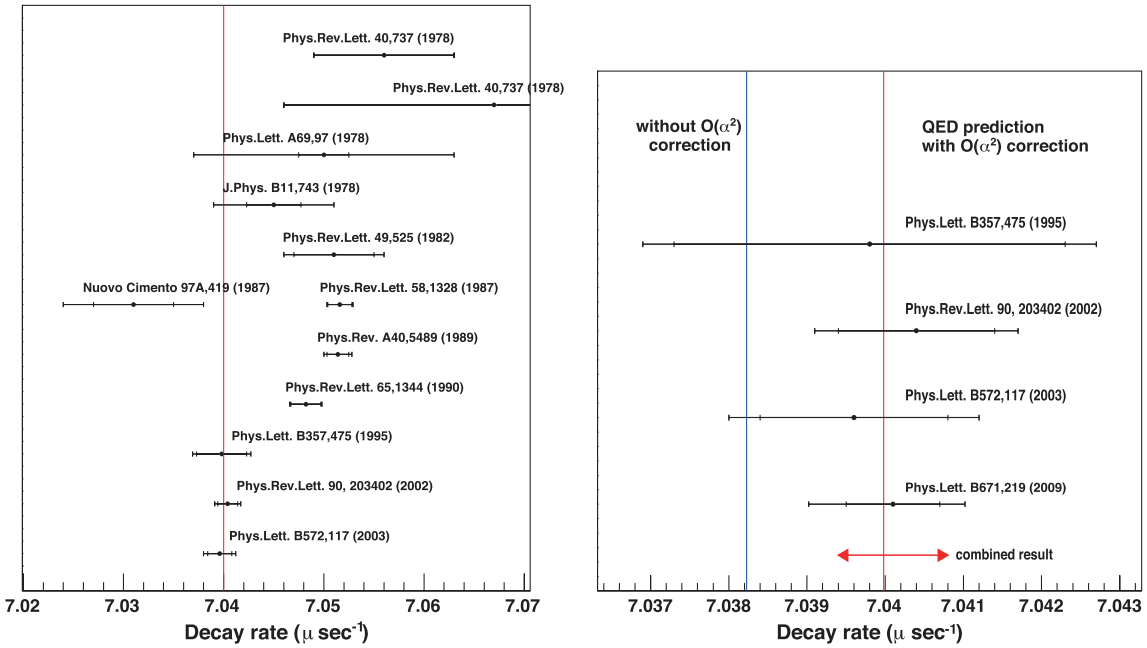

Fig. 3. (Left) History of the o-Ps lifetime measurements. The lifetime puzzle was solved by our measurements in 1995. (Right) Decay rates measured in the last four experiments and their combined result. The predictions of bound-state QED are also shown as lines. The combined result is consistent with the $\mathcal{O}(\alpha^2)$ correction. Republished with permission from [28].

and also confirmed the o-Ps lifetime consistent with the theoretical calculation. Four precise measurements [21,25–27] have been achieved by our group and the Michigan group, and the lifetime predicted with bound-state QED has been confirmed in an $\mathcal{O}(\alpha^2)$ order correction (Fig. 3).

3. Positronium hyperfine splitting interval

The energy levels of the ground states of o-Ps and p-Ps differ slightly; the difference is called Ps hyperfine splitting (HFS). Ps HFS is significantly larger (about 203 GHz) than hydrogen HFS (1.4 GHz) because of the following two reasons: (1) The magnetic moment is proportional to the inverse of the mass, thus a large spin–spin interaction is expected for Ps. (2) o-Ps has the same quantum number as a photon, thus o-Ps undergoes quantum oscillation through a virtual photon; o-Ps $\rightarrow \gamma^* \rightarrow$ o-Ps. This oscillation frequency of 87 GHz contributes only to the o-Ps, and makes Ps HFS larger.

The value of Ps HFS was first measured in 1952 as 203.2(3) GHz [29]. After the first measurement, the accuracy of the measurement was improved until the two most precise measurements achieved in 1974 and 1983 by the Yale group [30] and the Brandeis group [31,32], respectively. The results of these two groups are consistent, and the combination of them is 203.388 65(67) GHz (3.3 ppm). On the other hand, the accuracy of the theoretical calculation was worse than that of the experiments until the 1990s. A new calculation method including the higher-order correction was established and the second and third corrections were performed [33–35] in 2000. The current value of the QED prediction is 203.3917(6) GHz (2.9 ppm) and a significant discrepancy of 15 ppm (3.9σ) is observed. This might mean the existence of new physics beyond the standard model. A new light particle that weakly couples to electrons could explain this discrepancy. However, we should carefully check the possibility of systematic errors missed in all the previous experiments.

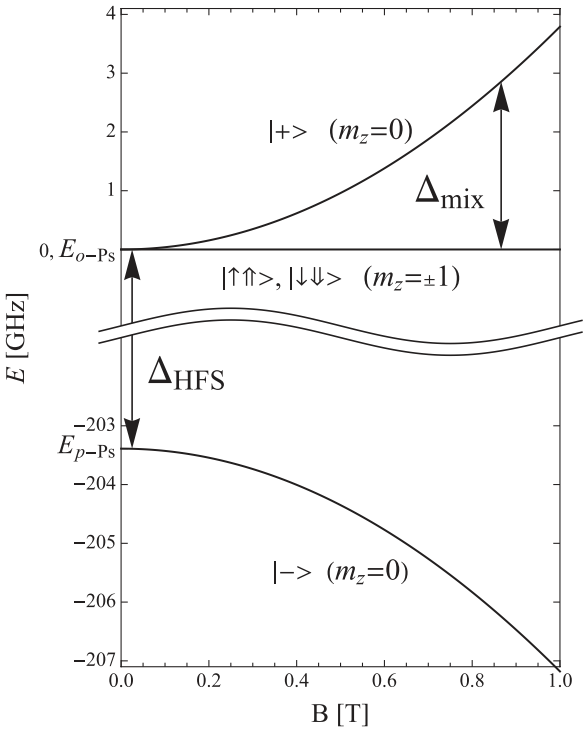

Fig. 4. Energy levels of Ps ground states under a static magnetic field. The arrows ↑, ↓ mean the spin of the electron, and ⇑, ⇓ means that of the positron.

3.1. Old experiments and systematic errors

Since it is difficult to produce and handle high-power 203 GHz millimeter waves, all previous Ps HFS measurements have been performed with an indirect method with a magnetic field. The static magnetic field causes Zeeman mixing between the $m_z = 0$ states of o-Ps and p-Ps, and the new mixed state, $|+>$, has an energy level that depends on the strength of the magnetic field strength and Ps HFS (Fig. 4). On the other hand, the $m_z = \pm 1$ state of o-Ps is constant under the magnetic field. The Zeeman shift between these two states was measured in all the previous experiments. They set an RF cavity filled with gas (N_2, Ar, He, etc.) under a static magnetic field (∼0.8 T). Inside the cavity, a β^+ source was attached, and Ps was formed in the gas. Changing the static magnetic field strength changes the Zeeman shift of Ps. When the shift matches the applied microwave RF frequency (∼2.3 GHz), o-Ps of $m_z = \pm 1$ transits to the $|+>$ state. $|+>$ immediately decays to back-to-back 511 keV γ rays, so the Zeeman resonance can be detected as the increase of 2γ decays as a function of the magnetic field strength. Since Ps is produced in the gas, the Ps collides with the gas molecule and the electric field of the gas molecule causes a shift in the energy state called the Stark effect. To estimate this effect (about 10 ppm for 1 atm gas), the previous experiments repeatedly measured Ps HFS at various gas pressures, and extrapolated HFS in the vacuum from the obtained values. This extrapolation is the same as in the lifetime measurements.

There are two possibilities for systematic errors in the previous experiments.

- In the 1970s and 1980s, the technology of superconductive magnets was not mature, and the previous experiments used normal magnets to make the static magnetic field. Due to the limited size of the magnets, non-uniformity of the magnetic field in the RF cavity was larger than about 10 ppm, and it was corrected for in their analysis. However, the errors of the magnetic field

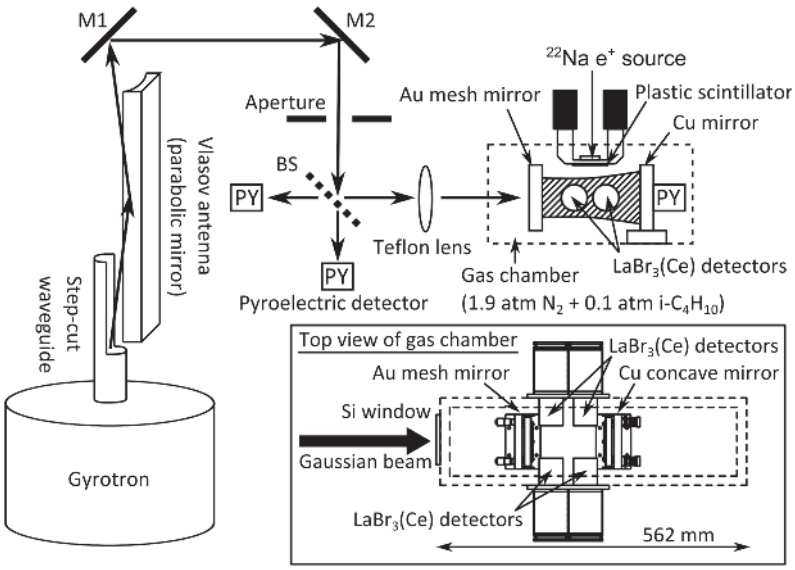

Fig. 5. A schematic view of the direct measurement of Ps HFS. Reprinted figure with permission from [38]. Copyright (2012) by the American Physical Society.

are enhanced and propagated on the final HFS results by a factor of 2. Non-uniformity of the magnetic field might cause the unknown sstematic errors.

- In the extrapolation procedure to correct for the Stark effect, Ps is assumed to be well thermalized, and the mean velocity of Ps is constant at all gas pressures. As shown in Sect. 2, this assumption causes a serious systematic error in the lifetime measurement. The HFS measurement would also be affected by this effect.

Recently, two new measurements using different methods have been made. One is measured via oscillations in the angular distribution of annihilation γ rays arising from quantum interference between o-Ps and p-Ps [36]. The other is a measurement of the difference between two Ps Lyman-α transitions using saturated absorption spectroscopy [37]. But neither of them have enough accuracy to clarify the discrepancy between the previous experiments and the theoretical calculation. We report our new two trials to examine Ps HFS.

3.2. Direct measurement of Ps HFS

Direct measurement of the HFS transition without a static magnetic field is completely free from systematic errors related to the magnetic field. The difficulty in direct measurement is the lack of a powerful light source, which overcomes the suppressed $M1$ transition (the transition rate is $3 \times 10^{-9}\,\mathrm{s}^{-1}$). We have developed a powerful millimeter-wave light source and successfully observed the direct transition. A schematic view of our experimental setup is shown in Fig. 5. The main components are as follows.

- **Gyrotron**: The gyrotron is a novel high-power radiation source for the sub-THz to THz frequency region. Cyclotron radiation from electrons emitted by the electron gun into a magnetic field is coherently enhanced in the resonant cavity of the gyrotron, and enhanced photons are emitted from its output window (Fig. 6). We use a gyrotron FU CW V, which produces 202.89 GHz radiation in TE_{03} mode in 15 ms pulses at 20 Hz [40]. Its output power is monitored and stabilized by a feedback system to the voltage of the heater of the electron gun. As a

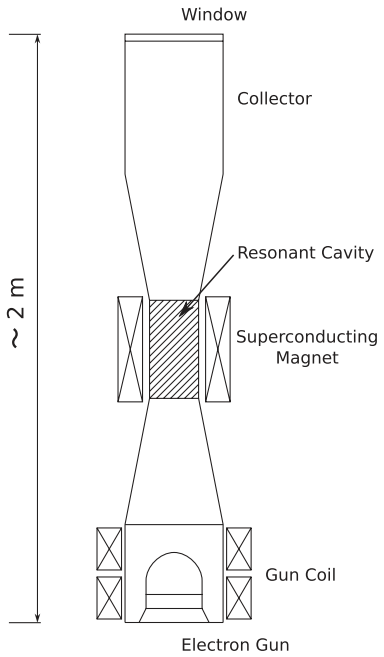

Fig. 6. A schematic of a gyrotron. Republished with permission from [39].

result, it can operate stably at about 300 W power within 10% fluctuation for more than a week. This long-time stable operation enables us to perform spectroscopy with a gyrotron.

- **Mode converter:** The TE_{03} mode milliwave radiation from the gyrotron is converted geometrically to a bi-Gaussian beam with a step-cut waveguide and a Vlasov antenna (a large parabolic mirror). Two parabolic mirrors after the antenna ($M1$ and $M2$) are used to convert the bi-Gaussian beam to a Gaussian beam. The power conversion efficiency of this converter is $28 \pm 2\%$ due to a limitation in the purity of the TE_{03} mode of the gyrotron output. The beam splitter (BS) splits the beam and its reflection from the cavity, and each power value is monitored with pyroelectric detectors (PY).
- **Fabry–Pérot cavity:** The Gaussian beam is accumulated in a Fabry–Pérot cavity made with a gold mesh plane mirror ($\phi = 50$ mm) and a copper concave mirror ($\phi = 50$ mm, curvature $=$ 300mm). The gold mesh plane mirror is made on a SiO_2 plate using photolithography and the liftoff technique. The mesh is designed with CST Microwave Studio, in which all materials are simulated, and the line width and separation are 200 μm and 160 μm, respectively, to obtain high reflectivity (99.38%) and reasonable transmittance (0.39%). When the cavity length (136 mm) is equal to a half-integer multiple of the wavelength of the milliwave light (about 1.5 mm), this cavity resonates and stores the beam. The cavity length is controlled by moving the copper concave mirror, which is mounted on a piezo-controlled stage (Nano Control TS102-G). The resonance of the cavity is monitored by a pyroelectric monitor, which is coupled with the cavity through a small hole ($\phi = 0.6$ mm) at the center of the copper concave mirror. From the width of the resonance peak against the cavity oscillation length, the finesse of the cavity is estimated as $\mathcal{F} = 623 \pm 29$ (Fig. 7). The power accumulated in the cavity reaches about 10 kW.
- **β tagging and γ detection system**: A 780 kBq ^{22}Na positron source is used for the Ps formation. The emitted positrons pass through a thin plastic scintillator (NE-102, thickness $=$ 0.1 mm) at the entrance of the cavity and produce light pulses. These light pulses are observed by two 2-inch

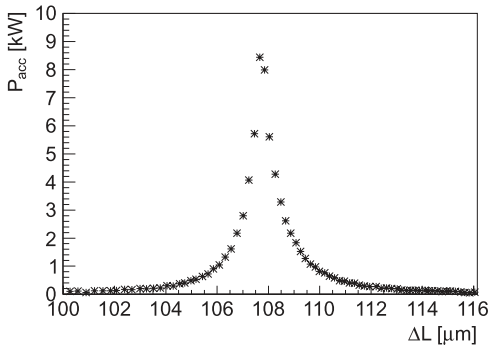

Fig. 7. The resonance curve of the Fabry–Pérot cavity. Republished with permission from [39].

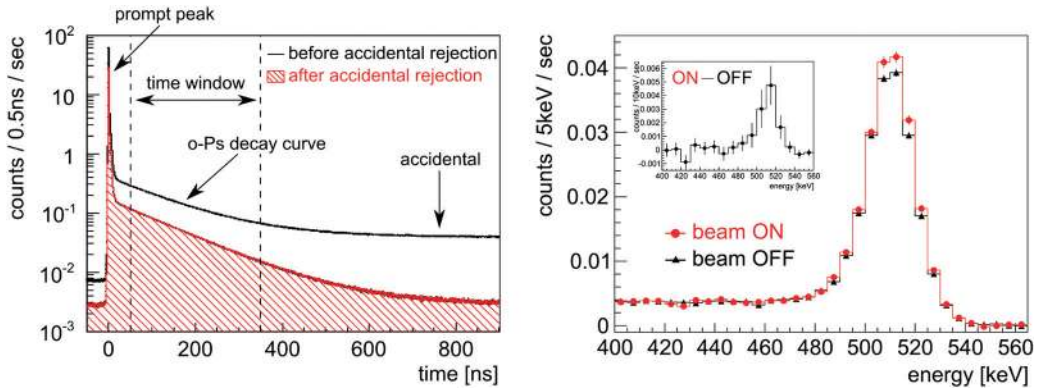

Fig. 8. (Left) Timing difference between the tag and the $LaBr_3$ scintillator. Timing window selection and pileup rejection are applied. (Right) The 511 keV peaks of the beam ON and beam OFF spectra. The difference between ON and OFF is also shown in the inset. A significant event excess is seen in the beam ON spectrum. Reprinted figure with permission from [38]. Copyright (2012) by the American Physical Society.

photomultiplier tubes (PMTs, Hamamatsu R5924-70), and the coincidence of these two PMTs is used as a tag for Ps formation. The cavity is filled with a gas mixture of 1.9 atm N_2 and 0.1 atm iC_4H_4. This gas component is optimized taking the Ps creation probability and the 203 GHz milliwave transparency into account. About 1/4 of the positrons form Ps in the cavity, and the γ rays from its decay are detected with four $LaBr_3$(Ce) scintillators ($\phi = 1.5$ inch, $L = 2.0$ inch). They are attached to four PMTs (Hamamatsu R5924-70), and their energy resolution is 4% (FWHM) at 511 keV. The time window is set from 50 ns to 350 ns for the timing interval between the tag and the $LaBr_3$ scintillators, and o-Ps-related events can be selected from the background events of positron annihilation. The energy of the tag scintillator is taken with long and short gates, and the ratio of the two gates is used for pileup rejection (Fig. 8 (left)).

With this setup, we have achieved the first observation of the direct transition of Ps HFS. All acquired data are separated into two categories, 'beam ON' and 'beam OFF', which reflect the duty cycle of the gyrotron, and the total period of data-taking is about two weeks. The energy spectra of the remaining events are plotted in Fig. 8 (right). A clear enhancement of 511 keV events can be seen in the beam ON spectrum. The difference between these two spectra is the component of the o-Ps $\rightarrow$ p-Ps transition, and its rate is $15.1 \pm 2.7(\text{stat.})^{+0.5}_{-0.8}(\text{sys.})$ mHz. The transition probability (or Einstein's A coefficient) can be calculated from this rate and the accumulated power of the 203

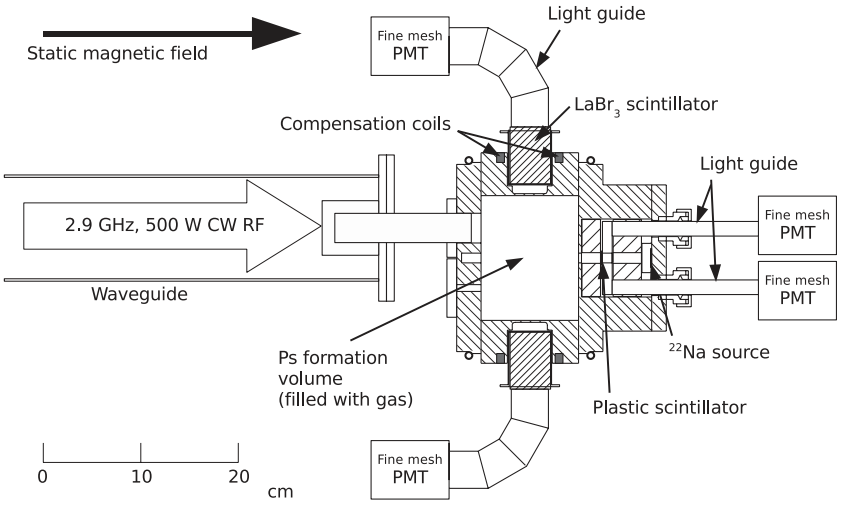

Fig. 9. The setup of the experiments (top view). These apparatuses are placed inside the bore of the superconducting magnet.

GHz millimeter wave ($11.0^{+3.6}_{-3.3}$ kW). The result is $A = 3.1^{+1.6}_{-1.2} \times 10^{-8}$ s^{-1}; this is consistent with the theoretical value of 3.37×10^{-8} s^{-1}[41].

After the success of this first observation, this experiment is on the next step, the first direct measurement of the Ps HFS value. A frequency-tunable gyrotron and a mesh mirror with a high power tolerance have been developed for the new measurement. Since the frequency of the gyrotron output is determined by its cavity size, the new gyrotron (FU CW G1) is designed for the easy replacement of its inner cavity. The cavity of FU CW G1 can be replaced without breaking the vacuum of the magnetron injection gun. All the necessary cavities have already been prepared. As for the Fabry–Pérot cavity, the material of the gold mesh mirror has been changed from a SiO_2 plate to a high-resistance silicon plate. Due to the bad thermal conductivity of SiO_2 (5 WK^{-1} m^{-1}), the mesh mirror used so far has melted away under the accumulated power of 20 kW. The new mirror, made of silicon, has good thermal conductivity (150 WK^{-1} m^{-1}) and is confirmed to be cooled with water under a power of about 25 kW.

The new measurement will be started this year, and the result with an accuracy of $\mathcal{O}(100\,\text{ppm})$ will be obtained within about a year.

3.3. New precision measurement of Ps HFS

The direct measurement of Ps HFS opens a new horizon for Ps measurement and milliwave optics, but more effort is needed to confirm the Ps HFS discrepancy of 15 ppm. The most promising way of testing the discrepancy is utilizing Zeeman mixing with a new experimental method. We have constructed a completely new experimental apparatus, taking special care over systematic errors.

Our apparatus is shown in Fig. 9.

- **Magnet**: A large-bore superconducting magnet is used to produce the static magnetic field $B \sim 0.866$ T. The bore diameter is 800 mm, and its length is 2000 mm. The magnet is operated in persistent current mode, making the stability of the magnetic field better than ± 1 ppm. A copper cavity for Ps creation is placed at the center of the bore, and coils wound around the cavity compensate for the slight gradient of the magnetic field. As a result, the uniformity of

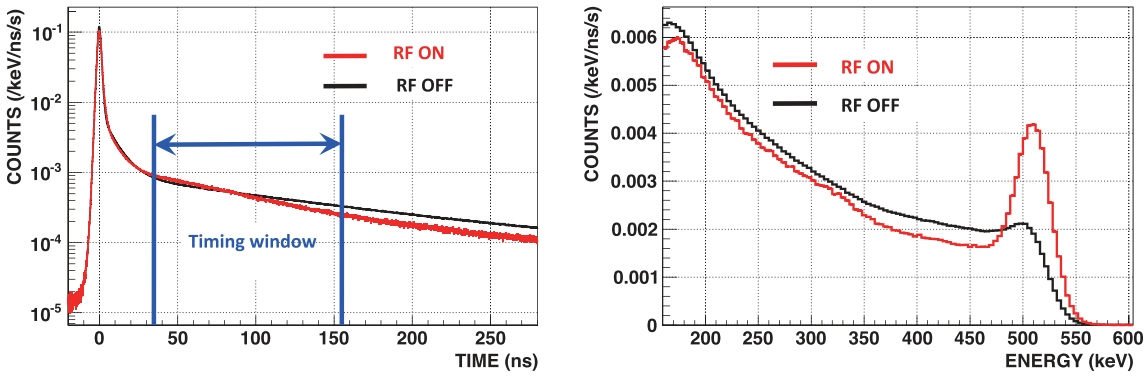

Fig. 10. (Left) Timing spectra with and without RF. (Right) Energy spectra of events inside the timing window. Events caused by the Zeeman transition cause a peak at 511 keV.

the magnetic field in the Ps creation region ($\phi = 40$ mm, $L = 100$ mm) is 0.9 ppm (RMS). This value is significantly improved from that of the previous measurements at the 10 ppm level.

- **Cavity and RF system**: Ps is created in the copper cavity, the size of which is $\phi = 128$ mm and $L = 100$ mm. The cavity is filled with pure $i\mathrm{C_4H_{10}}$ gas for Ps creation, and its pressure is tuned from 0.1 atm to 1.5 atm to evaluate the gas effect on Ps HFS. Before being filled with gas, the cavity is evacuated and baked at 60 °C for about a week to avoid water-vapor contamination.

  This cavity is also used as RF storage for the Zeeman transition. The size is tuned for a $\mathrm{TM_{110}}$ mode of 2.856 MHz RF (S band). The Q value of the cavity is about 11 000. A GaN amplifier is used to feed 500 W continuous RF to the cavity, and solid waveguides are used between the amplifier and the cavity for stable operation. The transmitted power and phase are monitored and stabilized with their feedback to the input of the amplifier.
- **β tagging and γ detection system**: The β tagging and γ detection system is similar to that for the direct HFS transition system described in Sect. 3.2. Positrons are fed from a ^{22}Na source (1 MBq), and pass a thin plastic scintillator (thickness = 0.2 mm), a signal from which is used to tag the Ps creation. The positron stops in the cavity, filled with $i\mathrm{C_4H_{10}}$ gas, forming Ps. Ps decays into photons that are detected with six $\mathrm{LaBr_3(Ce)}$ scintillators.

  As well as the direct measurement, the timing information on the interval between the β tag and γ ray enables us to select the Zeeman transition events from the prompt annihilation events. This improves the S/N ratio by a factor of about 20 compared to the previous measurements. Furthermore, we can select well thermalized Ps with the timing information. This means that one of the systematic problems, the nonlinear dependence of the Stark effect on the gas pressure, can be solved. The thermalization process in $i\mathrm{C_4H_{10}}$ gas is also studied in detail using another setup with a germanium detector.

The experiment was first performed in July 2010 and is ongoing. In Fig. 10, the measured timing and energy spectra with and without RF are shown. In the timing spectra, the events of Zeeman transitions increase at around 100 ns. These events are clearly shown in the energy spectra after the timing cut between 35 ns and 155 ns. The 511 keV peak caused by the Zeeman transition only appears in the RF-on spectrum. From the difference in the peak between RF-on and -off, the amount of the Zeeman transition is obtained. This value is scanned with the static magnetic field, and a Zeeman resonance curve is obtained, as shown in Fig. 11. From the center value of this resonance, we obtain the Ps HFS value in the gas. By changing the gas pressure, we obtain the dependence on the gas density. As shown in Fig. 12, we have already done many measurements at different pressures;

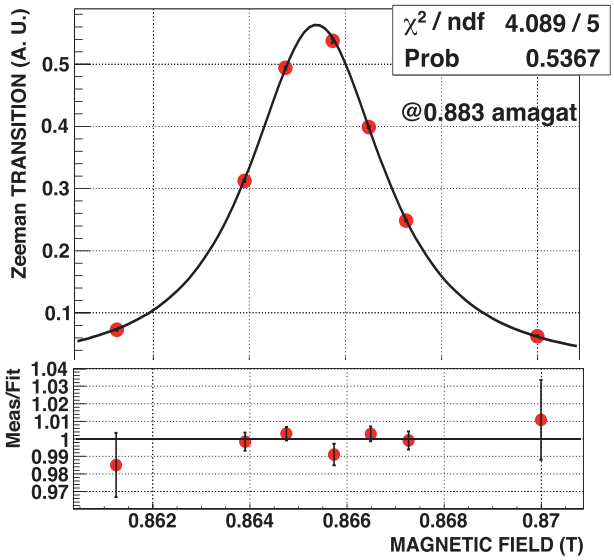

Fig. 11. Zeeman transition rate dependence as a function of the static magnetic field. From the center of this resonance curve, the Ps HFS value is calculated.

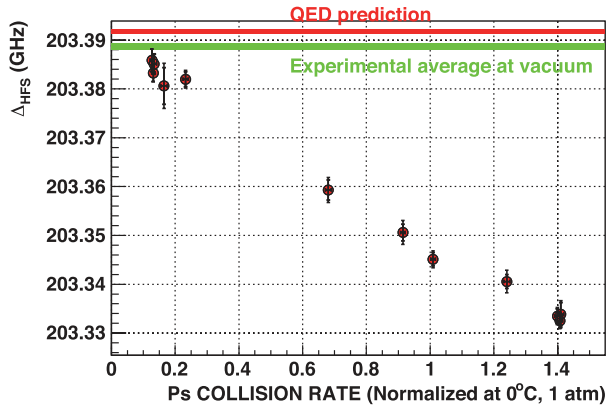

Fig. 12. Measured HFS values versus gas pressure. The bound-state QED prediction of $\mathcal{O}(\alpha^3 \ln \alpha^{-1})$ and the average result of the previous experiments are also shown.

however, it is not so simple to extrapolate the value at vacuum from these points. Although well thermalized Ps events are selected in our measurements, the nonlinear effect should be carefully checked at low pressure. Detailed analysis is ongoing, and the final results will be obtained next spring.

4. Summary

Positronium is an ideal system for the search for new physics beyond the standard model and research into bound-state QED. Many theoretical and experimental works have been done to investigate the properties of Ps. Two discrepancies between the theoretical calculations and the experimental values had been observed in the o-Ps lifetime and the ground-state HFS. The lifetime disagreement was identified as a systematic error in the experiments, but the HFS one is still unknown. We are trying to clear up this discrepancy with two new methods, direct measurement with the millimeter-wave technique and Zeeman measurement with timing selection. Each method will obtain results within a year.

Acknowledgements

I thank Prof. S. Asai for his useful comments and suggestions. Sincere gratitude is also expressed to Prof. T. Kobayashi, Dr T. Suehara, Dr T. Yamazaki, Mr A. Ishida, and Mr A. Miyazaki for useful discussions. Our HFS experiments are collaborative work between ICEPP, the University of Tokyo, KEK, and the University of Fukui. This work is supported by JSPS KAKENHI Grant Numbers 22340051, 23340059.

References

[1] S. G. Karshenboim, Phys. Rep. **422**, 1 (2005).
[2] S. G. Karshenboim, Appl. Surf. Sci. **194**, 307 (2002).
[3] T. Yamazaki et al., Phys. Rev. Lett. **104**, 083401 (2010).
[4] M. Skalsey and J. Van House, Phys. Rev. Lett. **67**, 1993 (1991).
[5] P. A. Vetter and S. J. Freedman, Phys. Rev. Lett. **91**, 263401 (2003).
[6] B. K. Arbic et al., Phys. Rev. A **37**, 3189 (1988).
[7] S. Asai et al., Phys. Rev. Lett. **66**, 2440 (1991).
[8] S. Orito et al., Phys. Rev. Lett. **63**, 597 (1989).
[9] T. Maeno et al., Phys. Lett. B **351**, 574 (1995).
[10] S. Asai et al., Phys. Lett. B **323**, 90 (1994).
[11] M. Tsuchiaki et al., Phys. Lett. B **236**, 81 (1990).
[12] A. Badertscher et al., Phys. Rev. D **75**, 032004 (2007).
[13] T. Mitsui et al., Phys. Rev. Lett. **70**, 2265 (1993).
[14] S. Asai et al., Phys. Rev. Lett. **66**, 1298 (1991).
[15] D. W. Gidley, J. S. Nico, and M. Skalsey, Phys. Rev. Lett. **66**, 1302 (1991).
[16] A. P. Mills Jr. and D. M. Zuckerman, Phys. Rev. Lett. **64**, 2637 (1990).
[17] K. Marko and A. Rich, Phys. Rev. Lett. **33**, 980 (1974).
[18] A. H. Al-Ramadhan and D. W. Gidley, Phys. Rev. Lett. **72**, 1632 (1994).
[19] K. Melnikov and A. Yelkhovsky, Phys. Rev. D **602**, 116003 (2000).
[20] B. Kniehl and A. A. Penin, Phys. Rev. Lett. **85**, 1210 (2000); **85**, 3065(E) (2000) [erratum].
[21] S. Asai, S. Orito, and N. Shinohara, Phys. Lett. B **357**, 475 (1995).
[22] C. I. Westbrook et al., Phys. Rev. Lett. **58**, 1328 (1987).
[23] C. I. Westbrook et al., Phys. Rev. A **40**, 5489 (1989).
[24] J. S. Nico et al., Phys. Rev. Lett. **65**, 1344 (1990).
[25] R. S. Vallery, P. W. Zitzewitz, and D. W. Gidley, Phys. Rev. Lett. **90**, 203402 (2002).
[26] O. Jinnouchi, S. Asai, and T. Kobayashi, Phys. Lett. B **572**, 117 (2003).
[27] Y. Kataoka, S. Asai, and T. Kobayashi, Phys. Lett. B **671**, 219 (2009).
[28] Y. Kataoka, *Test of Bound State QED Higher Order Correction: Precision Measurement of Orthopositronium Decay Rate*, Ph.D. Thesis, University of Tokyo (2007).
[29] M. Deutsch and S. C. Brown, Phys. Rev. **85**, 1047 (1952).
[30] M. W. Ritter et al., Phys. Rev. A **30**, 1331 (1984).
[31] A. P. Mills Jr. and G. H. Bearman, Phys. Rev. Lett. **34**, 246 (1975).
[32] A. P. Mills Jr., Phys. Rev. A **27**, 262 (1983).
[33] B. A. Kniehl and A. A. Penin, Phys. Rev. Lett. **85**, 5094 (2000).
[34] K. Melnikov and A. Yelkhovsky, Phys. Rev. Lett. **86**, 1948 (2001).
[35] R. J. Hill, Phys. Rev. Lett. **86**, 3280 (2001).
[36] Y. Sasaki et al., Phys. Lett. B **697**, 121 (2011).
[37] D. B. Cassidy et al., Phys. Rev. Lett. **109**, 073401 (2012).
[38] T. Yamazaki et al., Phys. Rev. Lett. **108**, 253401 (2012).
[39] T. Yamazaki, *Direct Measurement of the Hyperfine Transition of Positronium using High Power Sub-THz Radiation*, Ph.D. Thesis, University of Tokyo (2012).
[40] T. Idehara and S. P. Sabcevski, J. Infrared Milli. Terahz. Waves **33**, 667 (2012).
[41] P. Wallyn, W. A. Mahoney, P. H. Durouchoux, and C. Chapius, Astrophys. J. **465**, 473 (1996).